EUROPEAN FUSION DEVELOPMENT AGREEMENT

EFDA–JET–CP(06)03-11

I. Voitsekhovitch, R.V. Budny, E. Joffrin, H. Leggate, D.C. McDonald
and JET-EFDA Contributors

Energy, Particle and Momentum Transport in JET H-mode Plasmas and Hybrid Scenarios

Energy, Particle and Momentum Transport in JET H-mode Plasmas and Hybrid Scenarios

I. Voitsekhovitch[1], R.V. Budny[2], E. Joffrin[3], H. Leggate[1], D.C. McDonald[1]
and JET-EFDA Contributors*

[1]EURATOM/UKAEA Fusion Association, Culham Science Centre, Abingdon, OX14 3DB, UK
[2]Princeton Plasma Physics Laboratory, Princeton, New Jersey, PA, USA
[3]Association EURATOM-CEA, Cadarache, 13108, St Paul lez Durance, FranceResults and Future Perspectives",
Fusion Energy 2000 (Proc. 18th Int. Conf. Sorrento, 2000), IAEA, Vienna (2001).

Preprint of Paper to be submitted for publication in Proceedings of the
33rd EPS Conference,
(Rome, Italy 19-23 June 2006)

ABSTRACT

The Hybrid Scenario (HS), i.e. the regime with reduced or fully suppressed MHD activity (q_0>1) and generally high β_N (≥2.5)[1], is presently considered as an alternative scenario for improving the plasma performance beyond the conventional H-mode regime. However, the advantages of HS for plasma confinement are still an open question. The transport analysis of 10 JET H-mode plasmas performed in a broad density and q_{95} range[2] (Table I) and 7 HS performed at low density, q_{95}~4 and different triangularity[1, 2] (Table II) is presented here with the goal of (1) testing the theory-based transport models (MMM95[3] and GLF23[4]) and (2) comparing (when it is possible) the transport properties in these regimes. The interpretative analysis is performed with the TRANSP code[5]. The ASTRA code[6], with the GLF23 and MMM95 modules for anomalous transport and NCLASS module[7] for neoclassical transport, is used for predictive modelling. The modelling of each transport quantity (temperatures, density and momentum) is performed with prescribed other plasma profiles and sources from TRANSP simulations.

1. THERMAL TRANSPORT

Four HS and five H-mode plasmas within the same density range (n_l=(2.2-4.14)10^{19} m^{-3}, n^l is the central line averaged density) have been selected for the modelling of thermal transport. The results of modelling can be briefly summarised as follows: (1) the electron temperature is under-predicted in most shots while the ion temperature (T_i) is frequently over-predicted (Fig.1); (2) the prediction discrepancy obtained for T_i with the MMM95 model correlates with plasma density; (3) in a number of discharges the turbulence threshold inside r/a = 0.2-0.4 is overestimated with the GLF23 model, the modes are linearly stable leading to the strong overestimation of temperature with the remaining neoclassical transport. The correlation of the MMM95 prediction discrepancy with density can be displayed as a correlation with plasma β (=ratio of kinetic to magnetic pressure) (Fig.2). The results of JET are compared in this figure with the data of ASDEX-Upgrade where the improved H-mode plasmas (equivalent to HS at JET) are obtained at higher densities[8]. The modelling shows that the thermal ion confinement is worse than the MMM95 prediction in low β H-mode plasmas and HS of JET while some improvement with respect to this model is obtained at higher β on ASDEX-Upgrade. The unsatisfactory temperature prediction in JET H-mode plasmas and HS does not allow a comparison of thermal transport in these regimes through its comparison with the models. Dedicated experiments are needed for this purpose.

2. PARTICLE TRANSPORT

The electron density peaking in plasmas with q_{95}≅3-4 estimated with the Thomson scattering data in TRANSP increases by 15% with the reduction of ν* (in agreement with Ref.9) and saturates at low collisionality (Fig.3, closed circles). The peaking obtained at lowest collisionality in this group of shots (left closed circle) is reproduced in two similar discharges, although the error bars

are quite large as seen in Fig.3. One of the possible reasons limiting the density peaking is a strong sawtooth activity observed in these two discharges. The discharges performed at higher q_{95} have more peaked electron density n_e (open circles). The density peaking in four of seven HSs is larger than in H-mode plasmas performed at the same q_{95} (squares).

Three discharges with flat (61138), moderately peaked (61174) and peaked (61394) electron density profile have been selected for the modelling of deuterium density with the MMM95 model. It was found that the deuterium density peaking is strongly under-predicted in discharge 61174 while a better prediction accuracy is obtained for two other discharges with flatter deuterium density profile (Fig.4).

3. TOROIDAL MOMENTUM TRANSPORT

The momentum confinement time τ_φ estimated with TRANSP is similar to energy confinement time τ_E in HS and H-mode plasmas performed at $q_{95}\geq 3.7$ (Fig.5, left). The discharges performed at $q_{95}\cong 3$ have larger confinement times. The larger difference between τ_φ and τ_E in these discharges is obtained at lower plasma density while $\tau_\varphi \approx \tau_E$ at high density. The NBI torque used for the estimation of momentum transport consists of the collisional torque and JxB torque. In JET plasmas analysed here the contribution of the JxB torque is quite important varying from 30% at low n_e to nearly 80% at high n_e due to off-axis trapping of beam particles at high density. The largerτ_φ/τ_E-ratio is achieved in discharges performed with smaller JxB torque per particle (Fig.5, right). Interestingly, the ratio of local momentum (χ_φ) to thermal ion (χ_i) diffusivity does not always follow the ratio of confinement times – the χ_φ is smaller than χ_i even in discharges with $\tau_\varphi/\tau_E \approx 1$ (Fig.6) (see also [10]). The comparable thermal and momentum confinement times in these discharges are obtained in interpretative analysis due to smaller thermal electron transport (i) and/or steeper momentum profile (ii). In the examples shown in Fig.6 the inverse momentum scale length is much higher than the inverse ion temperature scale length ($R/L_m=19$, $R/L_{Ti}=4.96$, $R/L_{Te}=8$ at r/a=0.55 in 61132; $R/L_m=8.5$, $R/L_{Ti}=4$, $R/L_{Te}=7.4$ at r/a=0.55 in 61161). The code GYRO[11] was used for nonlinear simulations of the turbulent-driven fluxes and anomalous transport coefficients in discharge 61132. The calculation includes an extended radial domain and three kinetic species (bulk ions, combined impurity ions and electrons). It was found that the momentum diffusivity is indeed much lower than the thermal ion diffusivity ($\chi_\varphi=0.35$ m^2/s and $\chi_i=1.6$ m^2/s at r/a=0.65; compare to Fig.6).

The modelling of momentum transport in all discharges is performed with the GLF23 model. The linearly stable modes in the plasma core obtained with the GLF23 in a number of shots result in the strong over-prediction of core momentum with neoclassical transport[12]. The GLF23 prediction accuracy at mid-radius where the momentum transport is turbulent is shown in Fig.7 through the comparison of measured (CX) and calculated toroidal velocity. Quite accurate prediction (within 15%) is obtained in three discharges performed at low torque per particle (T/n_i) while the GLF23 model strongly over-predicts the plasma rotation (up to factor 5) at large T/n_i. This discrepancy is smaller but still significant for 5 HS performed at the same T/n_i as the H-mode plasmas.

SUMMARY

The results of interpretative analysis of 17 discharges can be summarised as following: (a) although the whole set of discharges scales inversely with collisionality[9], the subset of shots performed at q_{95}<4 shows a saturation of n_e-peaking at low ν^*, however, more experiments in this operational corner are needed to clarify this issue; the discharges with $q_{95} > 4$ and 4 of 7 HS have larger density peaking; (b) $\tau_\varphi \approx \tau_E$ in low density plasmas with $q_{95} \geq 3.7$ (both in H-mode and HS), the momentum confinement exceeds the thermal confinement in plasmas with $q_{95} \tilde{=} 3$ and low n_e; (c) χ_φ in gradient region is frequently below the thermal ion and sometimes effective diffusivity, i.e. the momentum profile is steeper than T_i-profile.

Although the theory-based models give a reasonable prediction of plasma profiles in some discharges, the overall agreement with experimental profiles is not satisfactory. The discrepancy obtained with the MMM95 model for T_i correlates with β. The density peaking is underestimated with this model. The GLF23 model shows that the drift modes are linearly stable in the plasma core in a number of discharges (although the uncertainty in the core magnetic shear may be large), the remaining neoclassical transport leads to a strong overestimation of core ion temperature and plasma rotation in these discharges. Thus, caution should be taken when applying these models to future reactor. Finally, the poor agreement with transport models does not allow a conclusion about the confinement advantages of HS with respect to the H-mode discharges performed at the same density and q_{95}.

Shot #	Bt, T/Ip l, MA	$q_{95}/\delta_{low}/\delta_{high}$	P_{nbi} MW	$S_{gas}/10^{21}$ part/s	$n_l/10^{19}$ m^{-3}	$T_{i0}/<T_i>$ keV	$T_{e0}/<T_e>$ keV
61132	1.9 / 2.35	2.8/0.18/0.23	2.5	0	2.3	3.6 / 1.5	3.4 / 1.6
61097	1.65 / 2	2.78/0.19/0.27	8	6	4.8	4.2 / 2	3.3 / 1.9
61174	1.9 / 2.35	2.78/0.19/0.27	12	11	5.6	4 / 2.3	4 / 2.2
61103	2.3 / 2.75	2.85/0.19/0.26	15	15	6.4	4.7 / 2.45	4.2 / 2.45
61138	2.25 / 2.5	3/0.37/0.44	14	46	8.25	2.8 / 1.5	3.1 / 1.65
61366	1.7 / 1.5	3.7/0.26/0.29	14	7.7	2.9	4.2 / 1.85	3.4 / 1.8
61543	1.7 / 1.5	3.75/0.29/0.3	14	7.9	4.14	4.2 / 1.86	3.4 / 1.7
61526	1.65 / 1	6/0.25/0.27	7.9	6.4	2.4	3.2 / 1.1	3 / 1.3
61520	2.3 / 1.4	6/0.24/0.27	14	14.5	3.1	4.1 / 1.9	3.7 / 2
61236	3 / 1	9 /0.22/ 0.27	12.5	2.8	2.3	4.5 / 1.4	4.4 / 1.5

Table I: Parameters of H-mode discharges

Shot #	Bt, T/Ipl, MA	$q_{95}/\delta_{low}/\delta_{high}$	P_{nbi}, MW	$S_{gas}/10^{21}$ part/s	$n_l/10^{19}$ m^{-3}	$T_{i0}/<T_i>$ keV	$T_{e0}/<T_e>$ keV
61387	1.7 / 1.4	3.8/0.14/0.28	13.6	3.8	2.2	4.7 / 2.1	3.5 / 1.9
61389	1.7 / 1.4	4.3/0.4/0.53	13.6	3.2	3.7	4 / 1.9	3.5 / 1.9
61392	1.7 / 1.4	3.5/0.4/0.48	13.6	3.2	3.4	4.7 / 2.2	3.6 / 2
61394	1.7 / 1.4	3.82/0.15/0.29	13.6	1.7	2.14	5.6 / 2.4	4.7 / 2
61161	2.4 / 2	3.75/0.14/0.28	15.5+1.5 ICRH	0	2.9	10 / 4.45	6.3 / 3.2
60931	1.7 / 1.4	4.1/0.4/0.5	17.7+2 ICRH	18.2	3.3	4 / 1.8	4.2 / 2.2
60927	1.7 / 1.4	4.1/0.42/0.5	14+1 ICRH	0	3.3	5.7 / 2.6	4.1 / 2.3

Table II: Parameters of Hybrid Scenarios

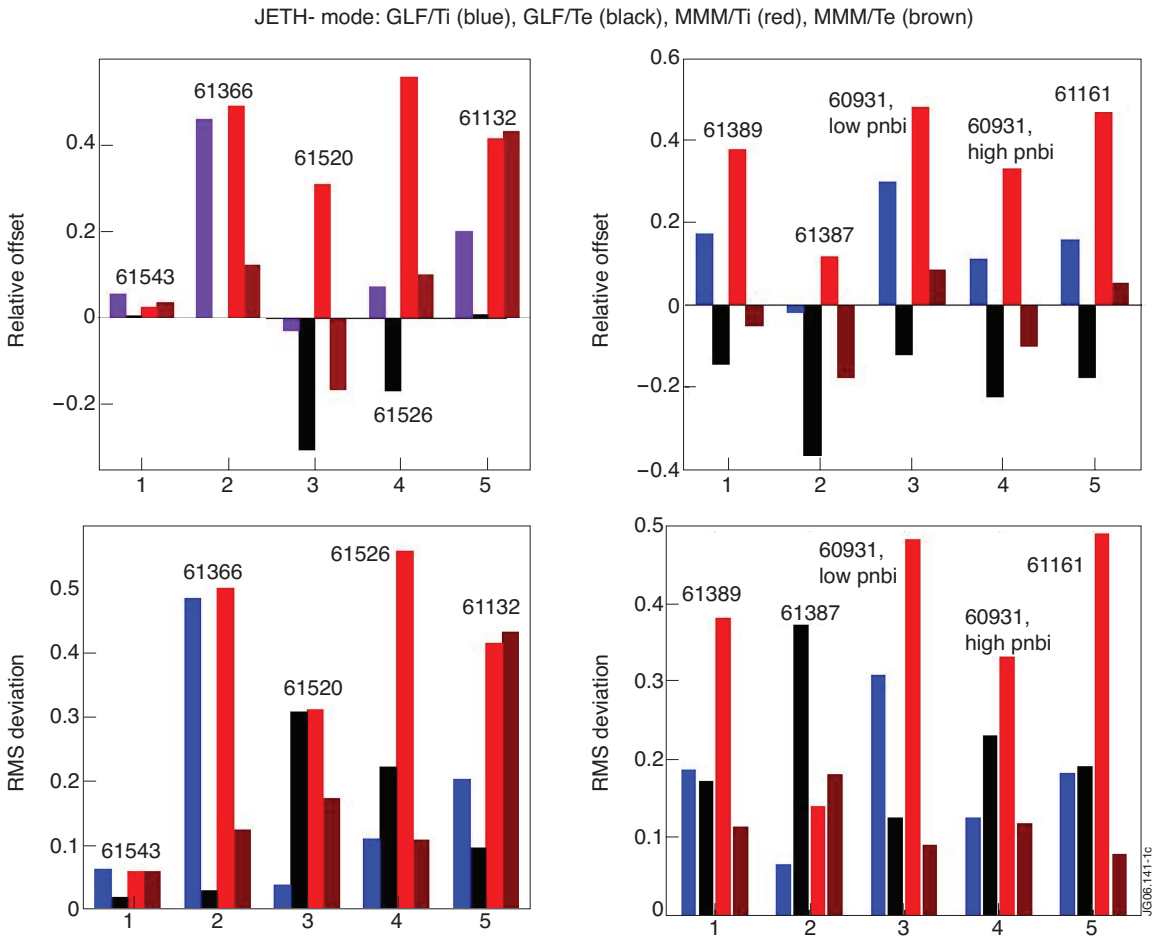

Figure 1: Relative offset=$\Sigma_j^N[(T_{sim}(r_j)-T_{exp}(r_j))/T_{exp}(r_j)]/N$ and RMS deviation=$\{\Sigma_j^N[(T_{sim}(r_j)-T_{exp}(r_j))/T_{exp}(r_j)]^2/N\}^{1/2}$ characterising the discrepancy between experimental and predicted profiles obtained with GLF23 (T_i (blue), T_e (black)) and MMM95 (T_i (red), T_e (brown)) models.

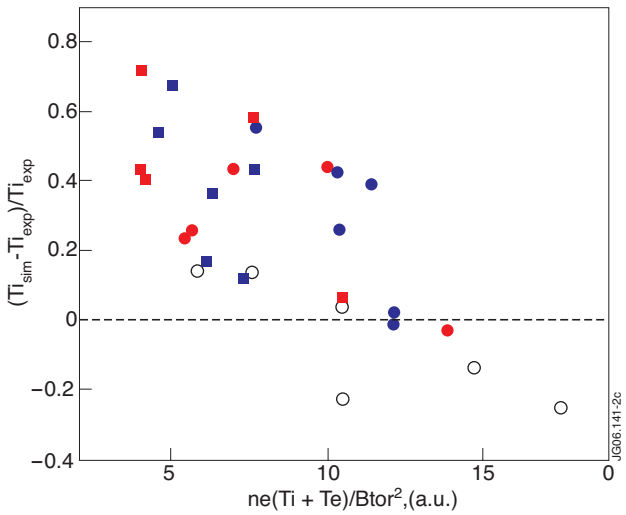

Figure 2: Discrepancy in ion temperature prediction with MMM95 model: H-mode (red), JET HS (blue), AUG improved H-mode (14521, 17870, 18882 (black)). Data are taken at r/a=0.2 (circles) and 0.5 (squares).

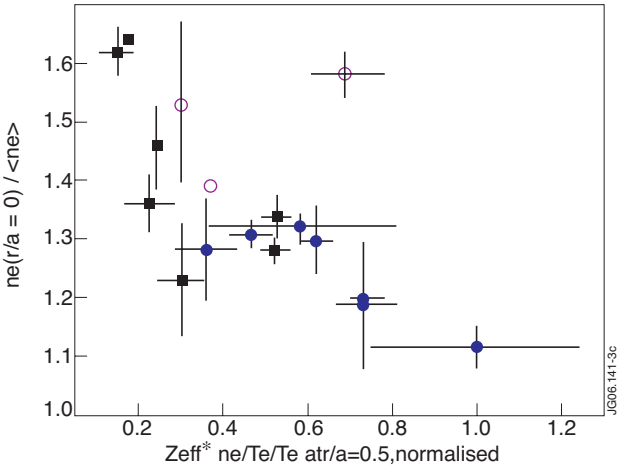

Figure 3: Electron density peaking with ν: H-mode with q_{95}<4 (closed circles), q_{95}≥6 (open circles), HS (squares). Error bars are determined by the largest deviation from the mean value during 1s.*

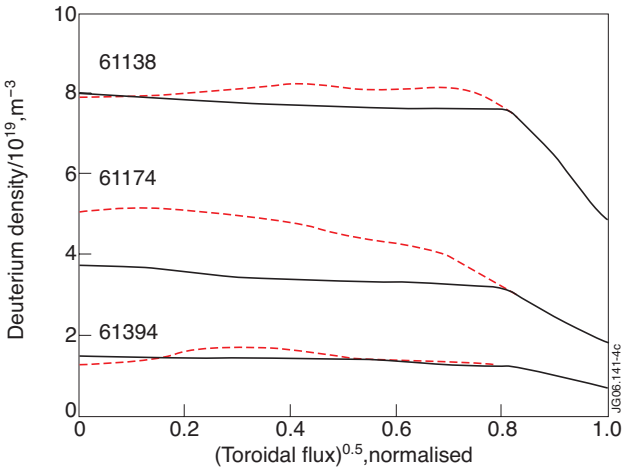

Figure 4: Deuterium density predicted with MMM95 model (solid) and estimated with TRANSP (dashed) for discharge with flat (61138), moderately peaked (61174) and peaked (61394) electron density profile.

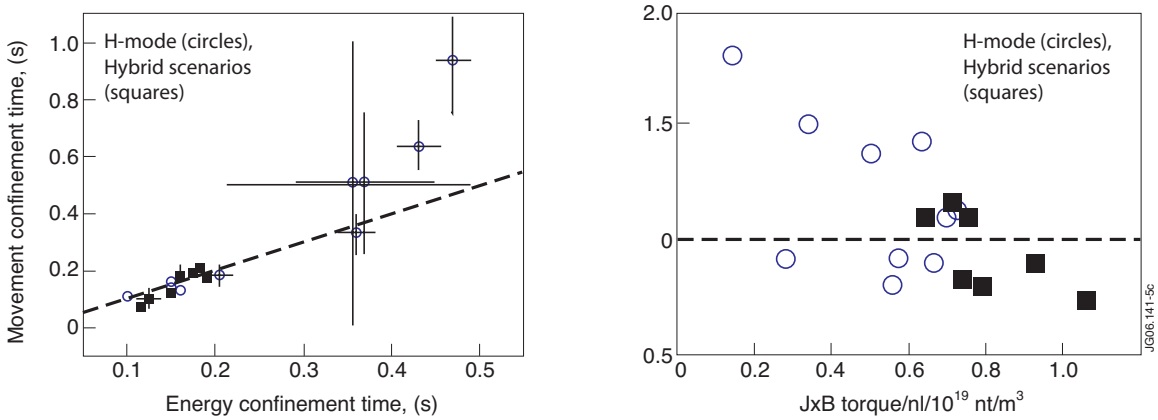

Figure 5: Momentum vs energy confinement time (left) and their ratio plotted as a function of JxB torque per particle (right).

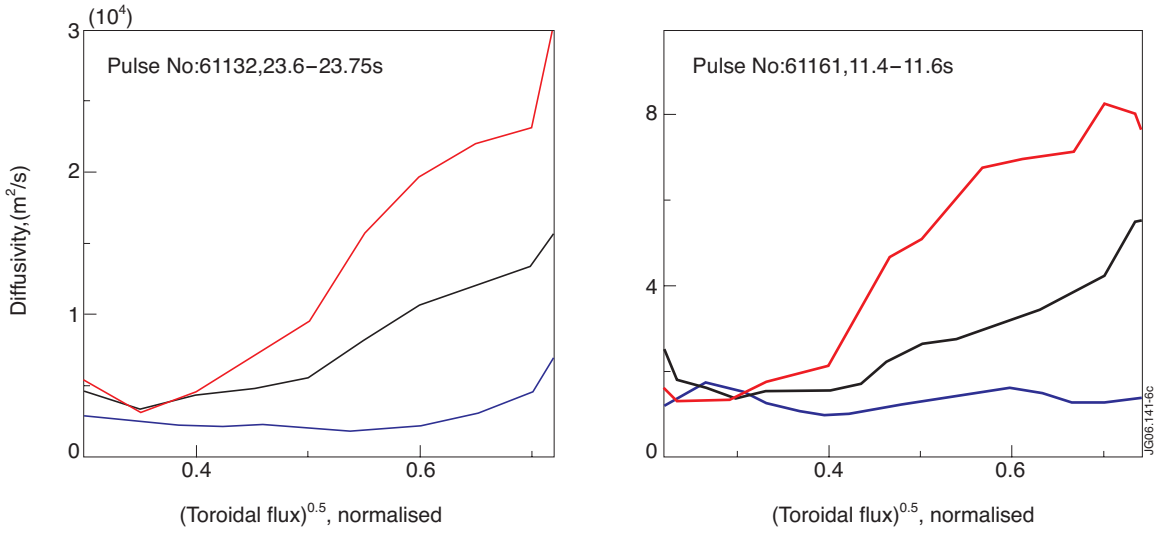

Figure 6: Momentum (blue), thermal ion (red) and effective (black) diffusivity in discharge with τ_φ/τ_E= 1.8 (left) and τ_φ/τ_E= 0.9 (right).

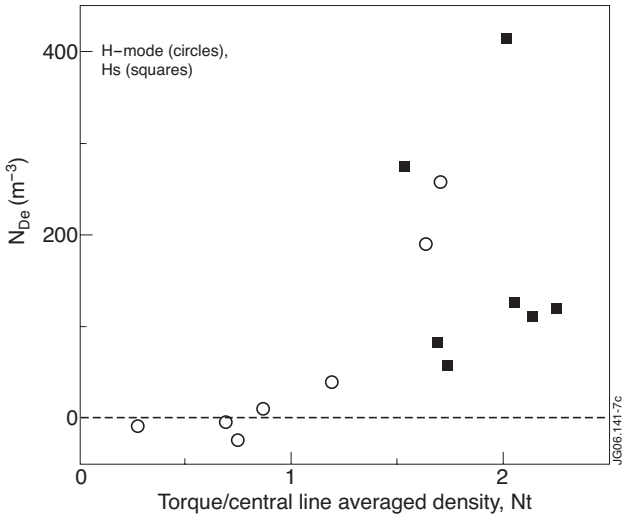

Figure 7: The discrepancy with GLF23 model at r/a=0.5 averaged over 1s during the stationary phase of discharge and plotted as a function of NBI torque per particle.